



Naval Research Laboratory

Washington, DC 20375-5000

NRL Memorandum Report 6623

AD-A223 207

Aureole Lidar: Ground Based Measurement

W. P. HOOPER

*Atmospheric Physics Branch
Space Science Division*

May 11, 1990

lo
1990

REPORT DOCUMENTATION PAGE

1a. REPORT SECURITY CLASSIFICATION UNCLASSIFIED		1b. RESTRICTIVE MARKINGS	
2a. SECURITY CLASSIFICATION AUTHORITY		3. DISTRIBUTION / AVAILABILITY OF REPORT Approved for public release; distribution unlimited.	
2b. DECLASSIFICATION / DOWNGRADING SCHEDULE			
4. PERFORMING ORGANIZATION REPORT NUMBER(S) NRL Memorandum Report 6623		5. MONITORING ORGANIZATION REPORT NUMBER(S)	
6a. NAME OF PERFORMING ORGANIZATION Naval Research Laboratory	6b. OFFICE SYMBOL (If applicable) Code 4110	7a. NAME OF MONITORING ORGANIZATION	
6c. ADDRESS (City, State, and ZIP Code) Washington, DC 20375-5000		7b. ADDRESS (City, State, and ZIP Code)	
8a. NAME OF FUNDING / SPONSORING ORGANIZATION Naval Research Lab non-specialfocus program	8b. OFFICE SYMBOL (If applicable) 5140	9. PROCUREMENT INSTRUMENT IDENTIFICATION NUMBER	
8c. ADDRESS (City, State, and ZIP Code) Washington, DC 20375		10. SOURCE OF FUNDING NUMBERS	
		PROGRAM ELEMENT NO. 61153N	PROJECT NO. RR031-03-4
		TASK NO. -	WORK UNIT ACCESSION NO. DN159-032
11. TITLE (Include Security Classification) Aureole Lidar: Ground Based Measurement.			
12. PERSONAL AUTHOR(S) Hooper, W.P.			
13a. TYPE OF REPORT Interim	13b. TIME COVERED FROM _____ TO _____	14. DATE OF REPORT (Year, Month, Day) 1990 May 11	15. PAGE COUNT 20
16. SUPPLEMENTARY NOTATION			
17. COSATI CODES		18. SUBJECT TERMS (Continue on reverse if necessary and identify by block number)	
FIELD	GROUP	SUB-GROUP	
		Lidar, Aureole, Lidar Investigation, Aerosol Extinction, Optical Depth, Laser Radar	
19. ABSTRACT (Continue on reverse if necessary and identify by block number)			
<p>An optical receiver (aureole) with a 50 milliradian field of view is used to measure the light reflected off a topographic target and forward scattered from aerosol particles back to the receiver. Simultaneously, a laser radar (lidar) backscatter profile is recorded. The aureole intensity provides a constraint of the inversion of lidar backscatter onto extinction profiles. A comparison between values of lidar reflection and aureole values is shown for data from 14 days. Atmospheric conditions on these days varied from extremely clear to fog and rain. Using the lidar/aureole relationship, four hundred consecutive lidar profiles are inverted into extinction profiles and displayed in a time-range false color display. This data was taken prior to the passage of a thunderstorm and reveals lidar's ability to observe the optical differences in small scale turbulent eddies.</p>			
20. DISTRIBUTION / AVAILABILITY OF ABSTRACT <input checked="" type="checkbox"/> UNCLASSIFIED/UNLIMITED <input type="checkbox"/> SAME AS RPT. <input type="checkbox"/> DTIC USERS		21. ABSTRACT SECURITY CLASSIFICATION UNCLASSIFIED	
22a. NAME OF RESPONSIBLE INDIVIDUAL W.P. HOOPER		22b. TELEPHONE (Include Area Code) (202) 767-3317	22c. OFFICE SYMBOL Code 4110

AUREOLE LIDAR: GROUND BASED MEASUREMENT

1. Introduction

Sunlight passing through thin clouds forms a bright disk called an aureole. Since Verdet's and Rayleigh's seminal works explaining how the scattering from small particles formed the disk, the aureole (on the rare occasions when it appears) can be utilized to understand the nature and approximate¹ size of cloud particles. At NRL, we are studying a similar phenomenon--a laser generated aureole. A narrow laser beam illuminates a rough surface (the ocean). The light is then reflected back over a wide range of angles and some of this reflected light is then scattered towards the laser creating a bright disk around the direct reflection spot. We have proposed using both the aureole and lidar return to estimate extinction profiles.

Using both analytical and Monte Carlo models of a laser beam aimed down towards the ocean from a satellite or aircraft, we have found that there should be a strong correlation between the optical depth and the magnitude of laser generated aureole.^{2,3} In fact, calculations of the aureole measured by a receiver having a large field of view (100 mrad) combined with theoretical lidar profiles using narrow field of view (10 mrad) indicate that the backscatter lidar profile with an aureole estimate of optical depth provides enough information to determine the extinction profile.

To experimentally test the aureole concept, a lidar system with both wide (aureole) and narrow (lidar) field of view receivers was located on a cliff overlooking the Chesapeake Bay, see Fig. 1. Both the laser and receivers are aimed at the NRL tower on Tilghman Island on the other side of the bay, 16 km away. Direct reflection and aureole signals are received from the tower and conifer trees behind the tower. With this system, we made measurements in a wide range of atmospheric conditions and tested the aureole concept.

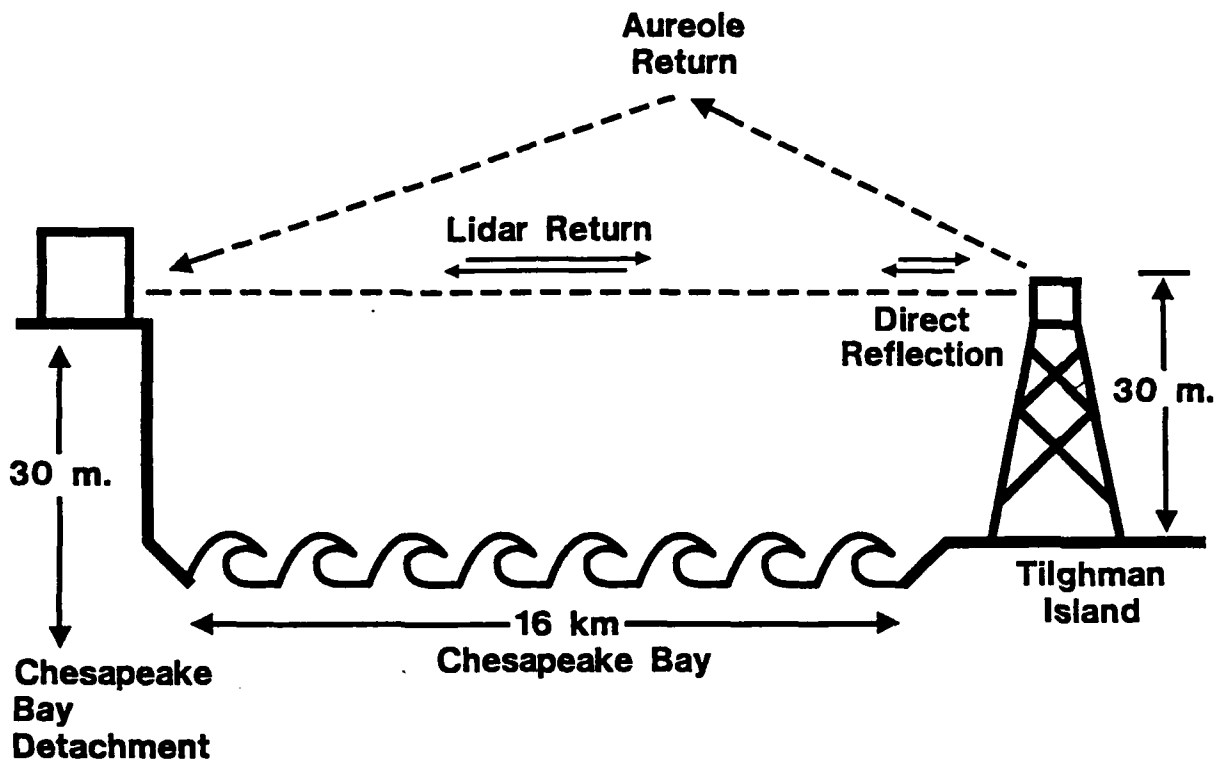


Figure 1. The aureole observations were made by aiming the laser at the tower across the bay. The narrow field of view receiver measures the backscatter as a function of range and the direct reflection off the tower, while the wide angle (aureole) receiver measures the light which is reflected at angle and forward scattered off aerosol particles towards the receiver.

2. Instrumentation

The Lidar-Aureole system (Table 1 and Fig. 2) has a pulsed laser transmitter (YAG at 1.06μ), a narrow field of view (10 mrad) receiver, and a wide field of view (50 mrad) receiver. Light pulses emitted by the laser are short (2.4 m in length) and highly collimated (0.5 mrad divergence). The narrow field of view receiver, a Cassegrainian telescope, collects primarily the light from the atmospheric backscatter and from light which directly reflected from the target. The aureole, aerosol backscatter, and target reflection signals are focused by a Fresnel lens (the wide field of view receiver). A beam stop in the focal plane blocks most of the aerosol backscatter signal and directly reflected light from the target. The remaining signal passes through a diffusing plate (o.d. 5 cm) which randomly redirects light and a lens that focuses some of the light onto a silicon avalanche photodiode.

While the design of the lidar receiver follows a traditional design, the aureole receiver design is new and comes from both experimental and theoretical considerations. Our theoretical models show that the aureole receiver should have a footprint of about 1 to 2 km in diameter at the target range. This footprint, which is largely independent of the target range, sets the receiver field of view. For our system, we want at least a 50 mrad field of view. After considering a number of telescopes, we selected a Fresnel lens. The lens are inexpensive and can have a f number of about one. The diffuse scatter off the lens surfaces represents a major problem that must be resolved by careful calibration and data processing.

The image size of the target footprint is several centimeters in diameter in the Fresnel focal plane and is too large for many detectors. After careful consideration of both Photomultiplier tubes (PMT) and silicon avalanche photodiodes, photodiodes were selected for the aureole detector. While the PMTs are 100 times larger in area than the photodiodes, the PMTs are 3 orders of magnitude less sensitive to 1μ radiation and are far more sensitive to visible radiation than photodiodes. Thus the photodiodes (unlike PMTs) are not swamped by sky noise and do not need narrow band-pass optical filters to block sky noise. This factor is especially important, since the aureole receiver has a wide field of view which makes narrow band pass optical filters hard to use and, for this reason, photodiodes were selected. A diffusing plate in the Fresnel focal plane solves the problem of the image size by redirecting the light onto a photodiode (o.d. 3mm) and allowing it to sample the signal from a large area (o.d. 5 cm).

Accurate aureole measurements require the separation of the directly reflected light from the aureole signal. Under many atmospheric conditions, the aureole signal is much weaker than the direct reflection. If even a small fraction of the directly reflected signal is scattered off the optics into the aureole detector, the aureole signal could be biased. Either the two signals can be separated spatially in the focal plane of the

TABLE 1 - LIDAR SYSTEM PARAMETERS

Transmitter	
Wavelength	1.06 microns
Pulse Duration	8 ns
Pulse Energy	750 mj
Beam Divergence	0.5 mrad
Pulse Repetition Rate	10 hertz
Lidar Receiver	
Collector	Cassegrainian Telescope (14" dia)
Sensor	Silicon Avalanche Photodiode
Amplifier	Logarithmic Amplifier (12Db)
Digitizer	12bit & 10 mhtz
Aureole Receiver	
Collector	Fresnel Lens (16" dia)
Sensor	Silicon Avalanche Photodiode
Amplifier	Logarithmic Amplifier (12db)
Digitizer	10 bit & 20 mhtz
Data Analysis Equipment	
Data Acquisition	Camac Crate
Analysis Computer	PDP 11/73
Display Computer	IBM PC Clone
Display Monitor	PGA monitor (256 Colors & 640x480 Pixels)
Data Storage	Magnetic Tape (Kennedy model 9100)

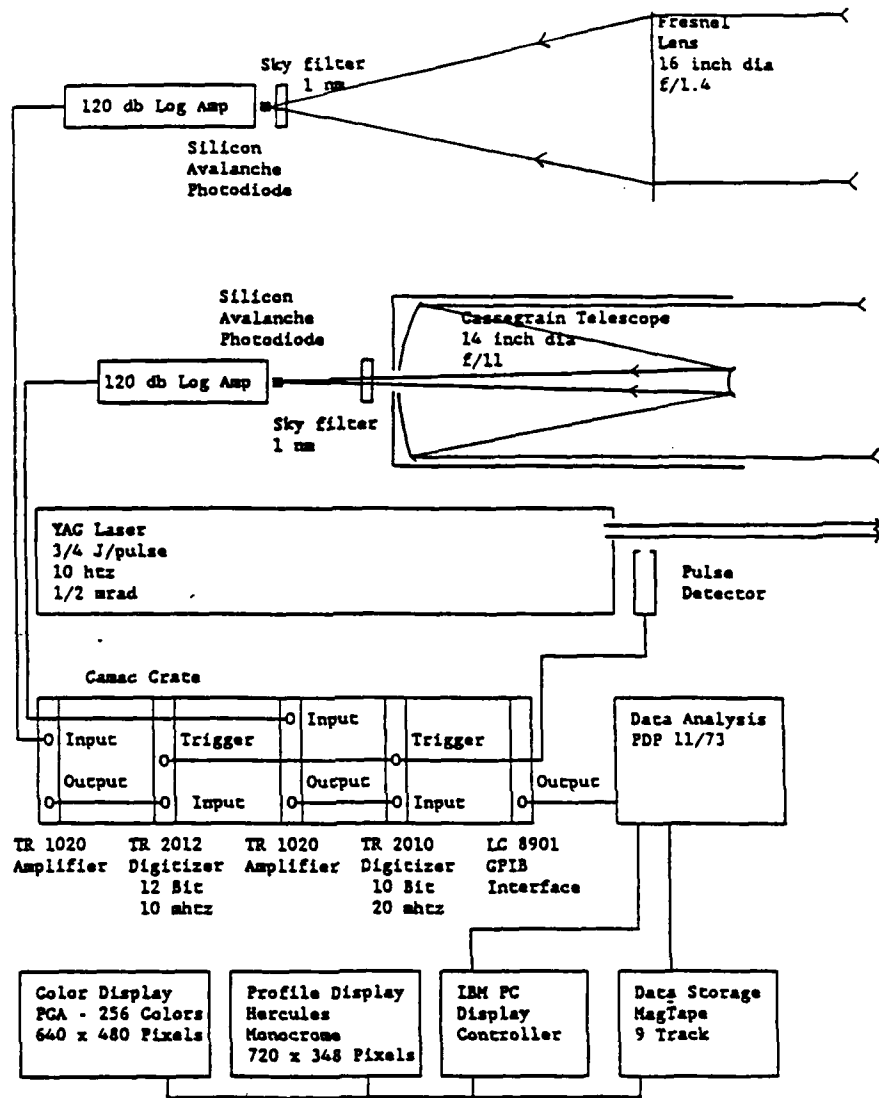


Figure 2. The lidar is illustrated in schematic form. A Fresnel collects the aureole signal from a wide angle, while the narrow field of view system uses a Cassegrainian telescope. Both signal focus on photodiode detectors with logarithmic amplifiers. The resulting analog signals are digitized signals and passed to the PDP-11/73. The final processed signals are displayed by the IBM using a Hercules monitor to display profiles and a PGA system to display false color time range displays.

receiver or the temporal separation between the arrival times of signals used to separate the signals. The second method requires a faster digitation rate than our present equipment allows and we are forced to rely on spatial separation; however in the future, we hope to use both methods to almost completely separate the signals.

Our initial aureole measurements showed near return (from inside 3 km range) and return from Tilghman Island. While the Tilghman Island return could be from the aureole, the near return in clear atmospheric conditions must result from the backscatter signal which is not blocked in the focal plane, instead reaches the detector after being scattered off the Fresnel lens, and represents cross talk between the direct and aureole returns. If the cross talk is solely dependent on the magnitude of the direct return signal (and thus the ratio of aureole to lidar signals are independent of range), then comparing the aureole and lidar measurements at near range with return from Tilghman Island provides the necessary information to estimate the magnitude of cross talk signal at Tilghman Island. Figs. 3 and 4 shows scatter plots of the aureole and lidar return for the same ranges for clear and very hazy conditions. The near return follow a simple curve. While (as the next paragraph will discuss) the relationship is not linear, still a simple one to one correspondence exists between the two signals. In both cases, the aureole to lidar ratio from Tilghman Island is larger than near return relationship. Also the aureole to lidar return ratio is much stronger under clear conditions than hazy conditions. (This relationship will be discussed more in the next section). These graphs provided the first indication that we were measuring more than just direct reflection.

To minimize the influence of extinction and laser energy variations, the aureole is normalized by the direct reflection. The aureole and lidar measurements are made simultaneously by different detectors, amplifiers, and digitizers and, therefore for the ratio the two signals to be observed, the differences between the two detector chains must be determined and removed by appropriate calibration constants. The calibration was done by reducing the return from Tilghman Island with neutral density filters. By comparing the strength of the aureole and lidar return with the transmission of the filter, power-law relationships are established (see Figs. 5 and 6):

$$P(R) = \exp \{ [S_1(R) - S_{1_0}] K_1 \} \quad (1)$$

and

$$A(R) = \exp \{ [S_2(R) - S_{2_0}] K_2 \}, \quad (2)$$

where

R is the range,
 $S_1(R)$ and $S_2(R)$ are the signals received from logarithmic amplifiers attached to the lidar and aureole detectors,
 S_{1_0} and S_{2_0} are the background signals,

$P(R)$ and $A(R)$ are the linear lidar and aureole signals, and K_1 and K_2 are the conversion factors derived from figs. 5 and 6. Since the logarithmic base of the logarithmic amplifiers are designed to compress the sensor voltages (and do not have a natural logarithm base), conversion factors are required to convert the signals to a natural logarithm base. Different digitation rates, digitation sensitivities, and optical alignments change the conversion factors. While the cross talk discussed in the previous paragraph introduces some noise to the aureole signal and must be removed, the cross talk does allow the aureole and lidar receiver signals to be compared on a shot by shot basis.

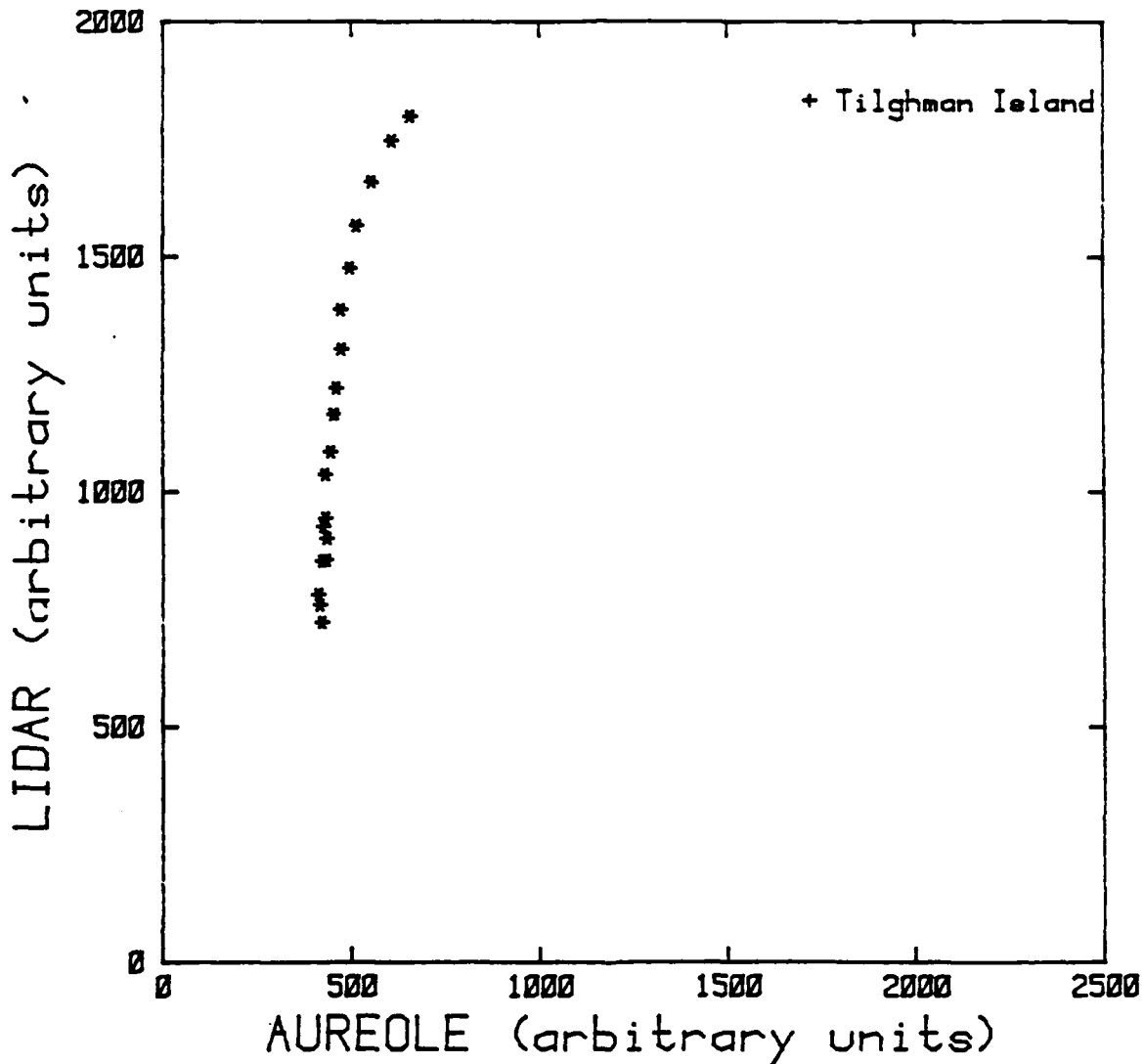


Figure 3. The uncorrected, near range return for the Lidar and Aureole sensors are shown. Data is from the very clear night of 5 Oct. 1988. The two logarithmic amplifiers have different logarithmic bases and this difference causes the nonlinearity between the returns. The aureole and lidar returns from Tilghman Island are shown by a cross.

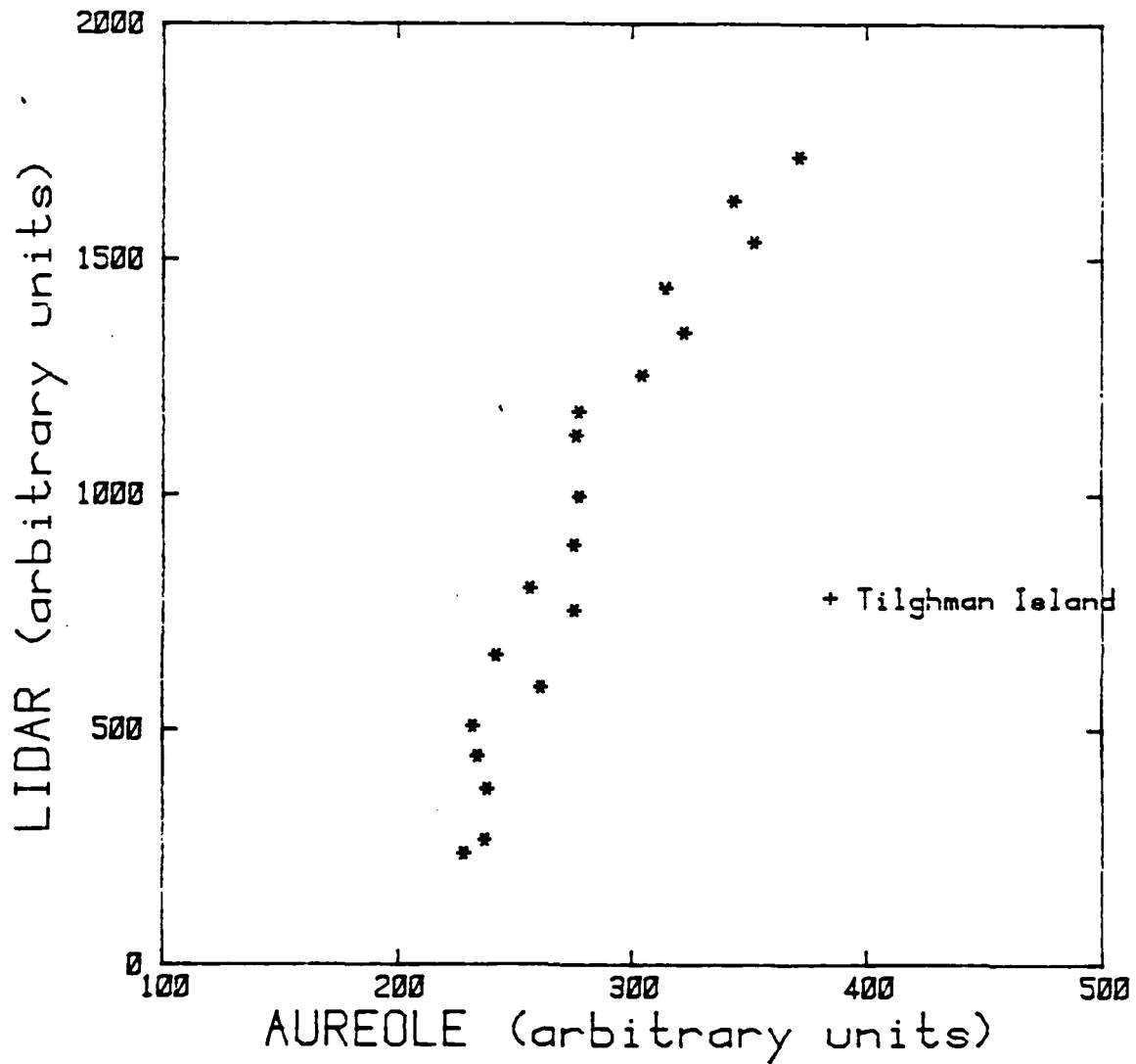


Figure 4. The comparison between Lidar and Aureole returns is illustrated for the hazy night of 3 Sept. 1988. The two returns from Tilghman Is are shown by the cross.

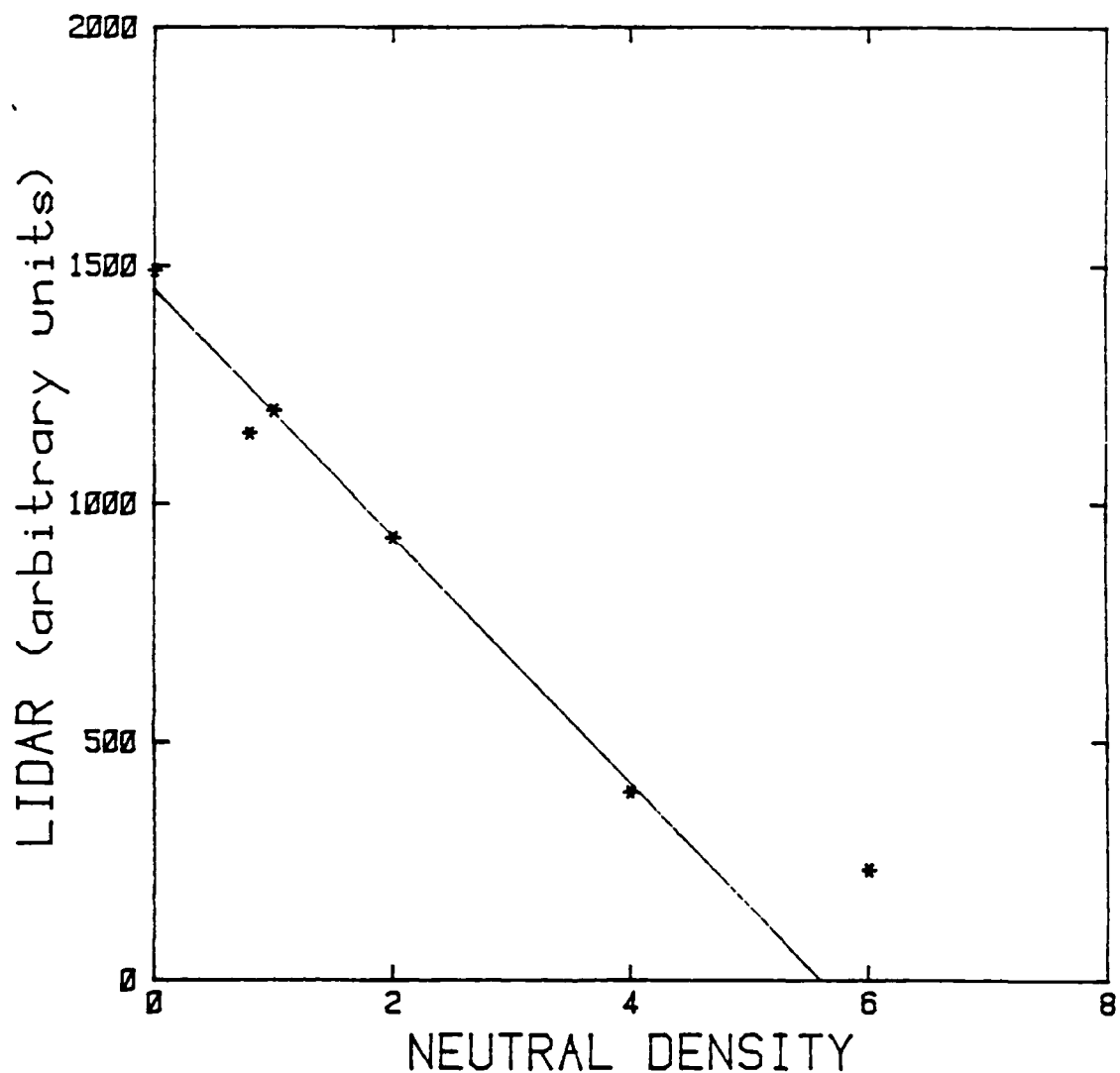


Figure 5. On an extremely clear night, neutral density filters were used to reduce the Tilghman Island lidar return and calibrate logarithmic amplifier. The straight line represents the fit to the data and was used to corrected the lidar data. At larger neutral density values the lidar signal does not go to zero. Instead, the lidar values are determined by the dark current of the sensor. Therefore, at higher densities the relationship between lidar and neutral density becomes non-linear and the value for a neutral density of 6 is not used in the least squares fit.

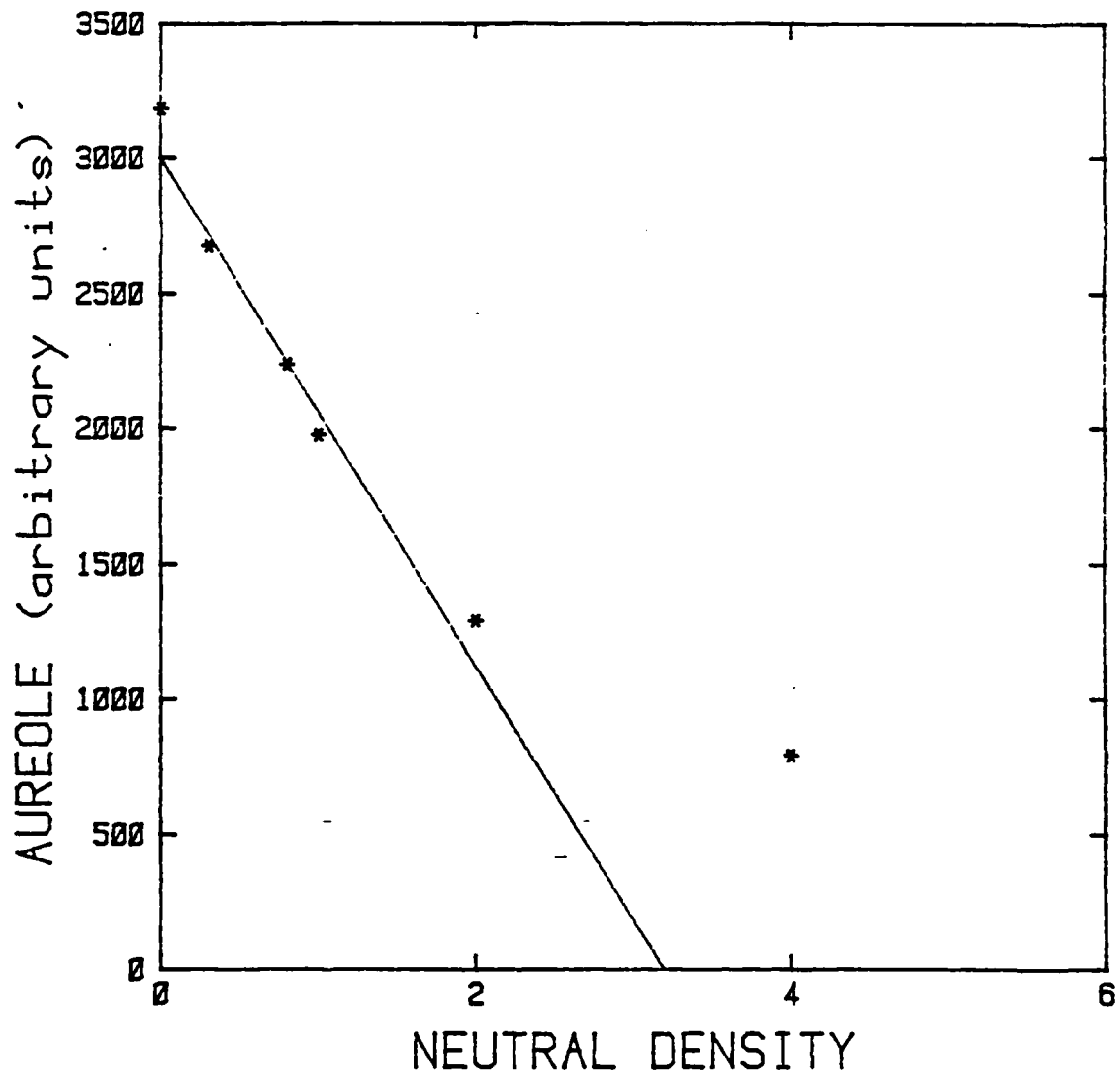


Figure 6. This plot is very similar to the one in figure 5 except the Aureole signal is calibrated with neutral density filters. In this case, the Aureole signal for neutral density of 4 was not used in the straight line fit.

3. Data Analysis

Lidar data can be analyzed to allow atmospheric aerosol structure to be observed remotely. Over short range intervals (<1 km), they are extremely sensitive to small changes in backscattering properties. However, extinction properties become extremely important over longer range intervals. The standard lidar equation is⁴:

$$P(R) = k F(R) \beta(R) \exp(-2 \int_{R'=0}^{R'=R} \sigma(R') dR') / R^2, \quad (3)$$

where

P is the power received,

k is system constants,

F(R) is the overlap function,

β is volume backscatter coefficient, and

σ is volume extinction coefficient.

The system received by the NRL lidar system is:

$$S_i(R) = \text{Log}(k F(R)) + \text{Log}(\beta(R)) - \int_{R'=0}^{R'=R} [\sigma(R') dR'] / K_1 - 2 \text{Log}(R), \quad (4)$$

where Log is a logarithm with a base of $\exp(K_1)$. If a power law relationship between extinction and backscatter is assumed and the overlap function is independent of range, the lidar signal can be converted to an extinction profile⁵. For our case, a linear backscatter to extinction relationship was assumed:

$$\beta = C \sigma. \quad (5)$$

In our calculations, the power law constant is assumed to be one. Using Eqs. (4) and (5), the extinction can be derived:

$$\sigma(R) = \exp\{[S_i(R) - S_i(R_0)] / \{1/\sigma(R_0) - \int_{R'=R}^{R'=R} [\exp\{S_i(R') + S_i(R_0')\}] dR'\}\}, \quad (6)$$

where R_0 is the range used for the boundary condition. For this paper, the boundary condition was set at 2 km. Equation (6) provides extinction for ranges from 2 km back towards the receiver. The following equation slightly modified from Eq. (6) allows the extinction to be calculated from 2 km out to 5 km⁶:

$$\sigma(R) = \exp\{[S_i(R) - S_i(R_0)] / \{1/\sigma(R_0) + \int_{R'=R_0}^{R'=R} [\exp\{S_i(R') - S_i(R_0')\}] dR'\}\}. \quad (7)$$

Equations (6) and (7) represent the standard Riccati or Bernoulli solution to the lidar equation. The accuracy of this solution rests strongly on the accuracy of the boundary condition, $r(R_0)$ and $S(R_0)$. For this constraint, a nonlinear relationship between aureole and extinction was determined experimentally (as will be discussed in the next section):

$$\tau = \int_{R'=R_2}^{R'=R_1} \sigma(R') dR' = 3.1 + \frac{3.1}{(A_0/P_r - 3.2)}, \quad (8)$$

where

P_r is the direct reflection from Tilghman Island,

A_0 is the aureole signal from Tilghman Island,

τ is the optical depth estimate,

R_1 and R_2 are maximum and minimum ranges.

Equation 9 based solely on an eyeball fit to the data and did not involve any theoretical calculations. Equation (8) provides a constraint on Eqs. (6) and (7):

$$\epsilon > \left| \tau - \int_{R'=R_2}^{R'=R_1} \sigma(r) dr \right|, \quad (9)$$

where ϵ is an arbitrarily small number (typically 10^{-5}). The final profile of extinction was found by varying boundary condition in Eqs. (6) and (7) and using a bisection routine to find the best boundary condition to fit Eq. (9). Of course, this boundary condition is not the 'real' value of extinction at range R_0 and the value compensates for other errors in the lidar return and inversion technique.

4. Measurement

For fourteen days, both the aureole and lidar returns were simultaneously measured. Fig. 7 shows a comparison of the aureole normalized by the reflection and the direct reflection. Each point represents an average of about two thousand pulses over 5 minutes. (While individual returns could be used, the time average minimizes the influence of small scale structure on the aureole.) The direct reflection displayed on the abscissa is the raw output of the lidar sensor. This output is logarithmic and, if the Tilghman Island reflection coefficient is constant, the return should be proportional to extinction. The ordinate is the normalized aureole combining both the raw aureole and lidar signals which is corrected for background signals and for the logarithmic base of the amplifiers. The aureole-reflection relationship observed is non-linear and suggests that the aureole is larger for clear conditions and weaker when the atmosphere is hazy.

For the horizontal laser beam used for our measurements, the observed relationship differs from our theoretical results for a down-looking lidar system. Since our aureole measurements are made at long range allowing the aureole signal to be contaminating by the direct reflected signal, these differences are to be expected. Many of the photons received from Tilghman Island undergo just the one reflection event off Tilghman Island. However, with the long horizontal path, some photons are forward scattered in narrow angles and do not leave the beam, while others re-enter the beam after scattering and reflection events. (This problem is quite different from the cross talk problem discussed in the previous section and, unlike the cross talk, increases with range.) Since the forward scattering is larger for hazy conditions than for clear conditions, the 'aureole' contribution to direct reflection also increases with extinction.

The resulting normalized aureole is, therefore, smaller for hazy conditions than for the clear conditions. Thus the aureole-extinction relationship for a long horizontal path is reversed from the relationship predicted by the models for vertical paths where aerosol is restricted to a thinner surface layer. This problem can be partially corrected by better temporal separation of the aureole and direct reflection signals. Interestingly, as we will show in the later this section, the measured aureole-reflection relationship can still be used to invert the lidar backscatter into extinction.

In earlier theoretical studies, we found that an accurate estimate of optical depth (or extinction) could be used to improve the inversion accuracy of lidar backscatter profiles into extinction profiles. The observed reflection-aureole relationship can also be used to constrain a Riccati lidar inversion. Under many conditions, the inversions yielded reasonable results. (Rain, strongly inhomogeneous structures, or foggy conditions did caused large errors.)

Fig. 8 shows a original profile and the same profile after being inverted. While the inverted profile appears "noisy", the false color plot of profiles (fig. 9) reveals the peaks and valleys continue from shot to shot outlining atmospheric structures. Fig. 9 contains 360 profiles with each profile having extinction values at 370 range intervals. The extinction values converted into an integer from 0 to 47 and displayed as a colors for the display. This figure represents an ultimate goal of the lidar inversion process--the ability to map extinction in space and time. The analysis reveals small scale atmospheric details just prior to and during the passage of a gust front. The individual lidar profiles resolve features down to 15 m with a time separation of 3s between profiles. Winds (about 10 m/s) were from the west along the lidar beam and, thus, from the lidar site out across the bay. The bottom of the boundary layer separates from the surface as it flows off the 30m cliff at the lidar site out over the bay and forms a large roll eddy which traps aerosols blown off the shore. At a range of 2 km, the flow interacts with the surface again forming small scale eddies. Near the end of the time series, the gust front passes the lidar site (at about 25 m/s). The structures are blown across the bay and rain begins at the lidar site. Unfortunately, as the gust front passed, power lines were knocked down and lidar measurements ceased.

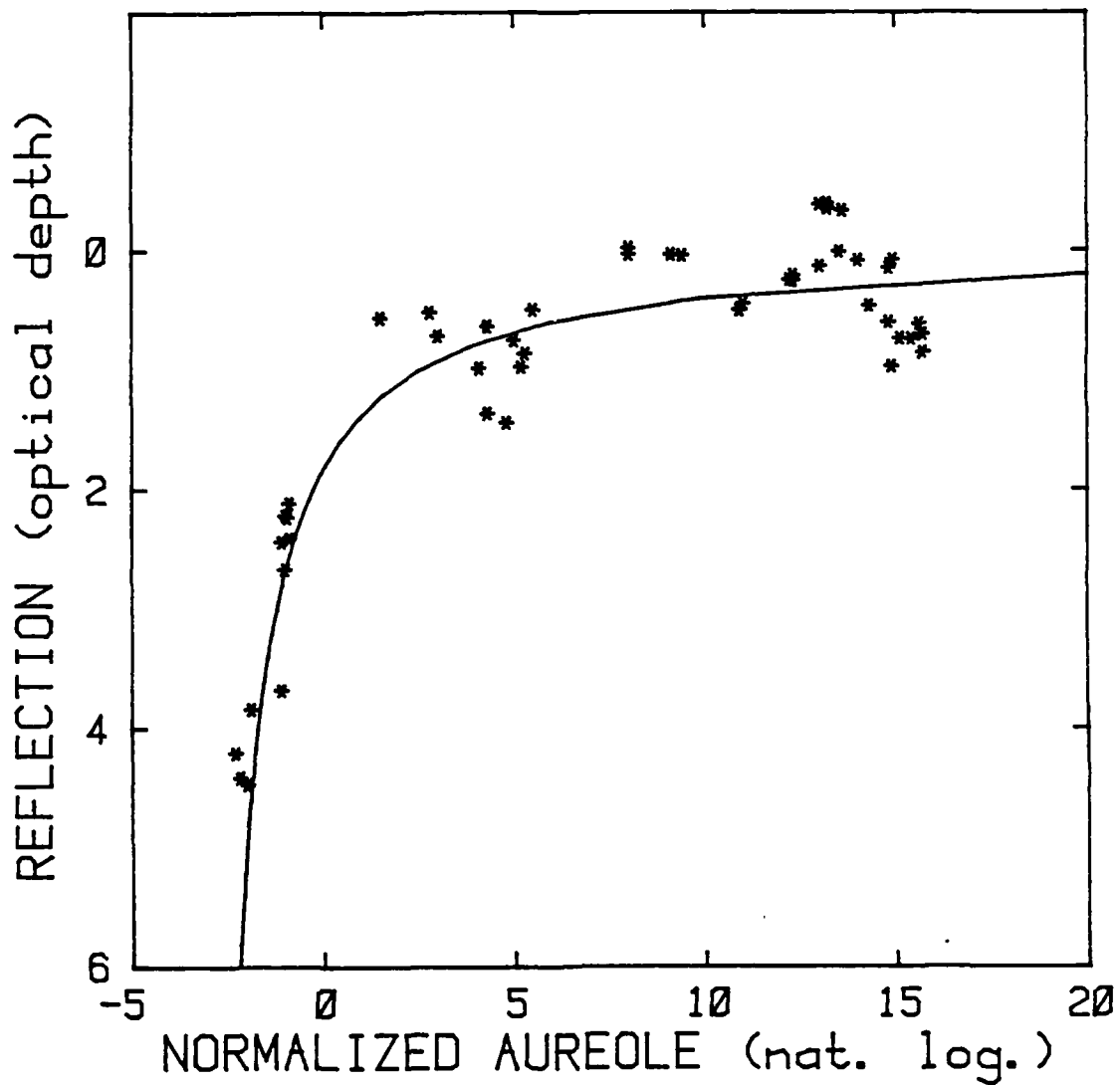


Figure 7. The Tilghman Island reflection and the normalized aureole from the Island are compared. The reflection is determined from the lidar return and the aureole is normalized by the reflection. This data is from 14 nights. Since the atmospheric conditions changed during the nights, more than one comparison between reflection and aureole was made each night. The solid line represents the eyeball fit to the data that was used to convert aureole values to optical depth.

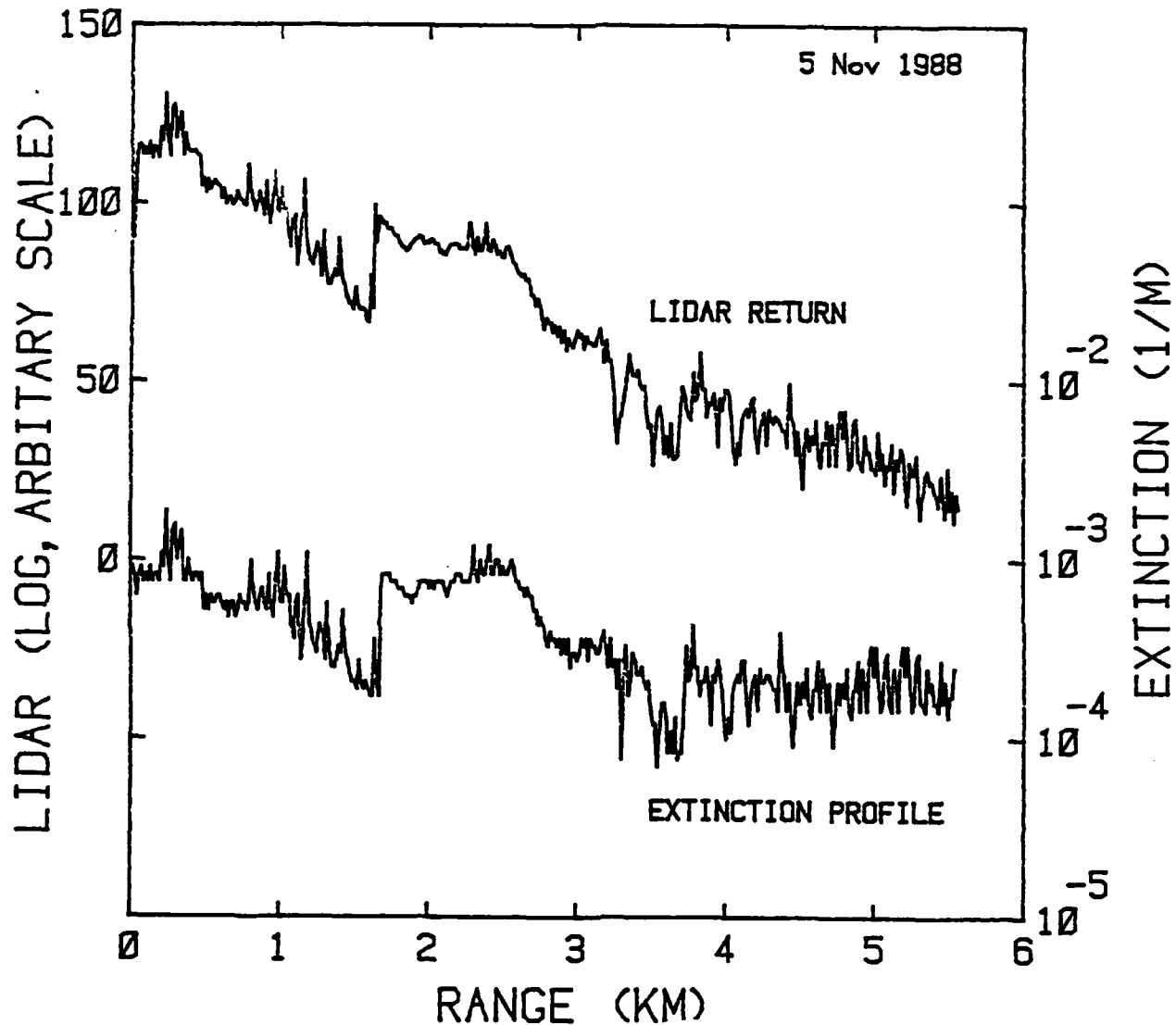


Figure 8. The same lidar profile is shown twice. One represents raw data that is only range corrected. The other shows raw data converted into extinction by a Riccati inversion. The data was taken just before the end of measurement period. The near return is from rain and the jump in the return at 2 km show the optical change during the passage of a rapidly moving gust front.

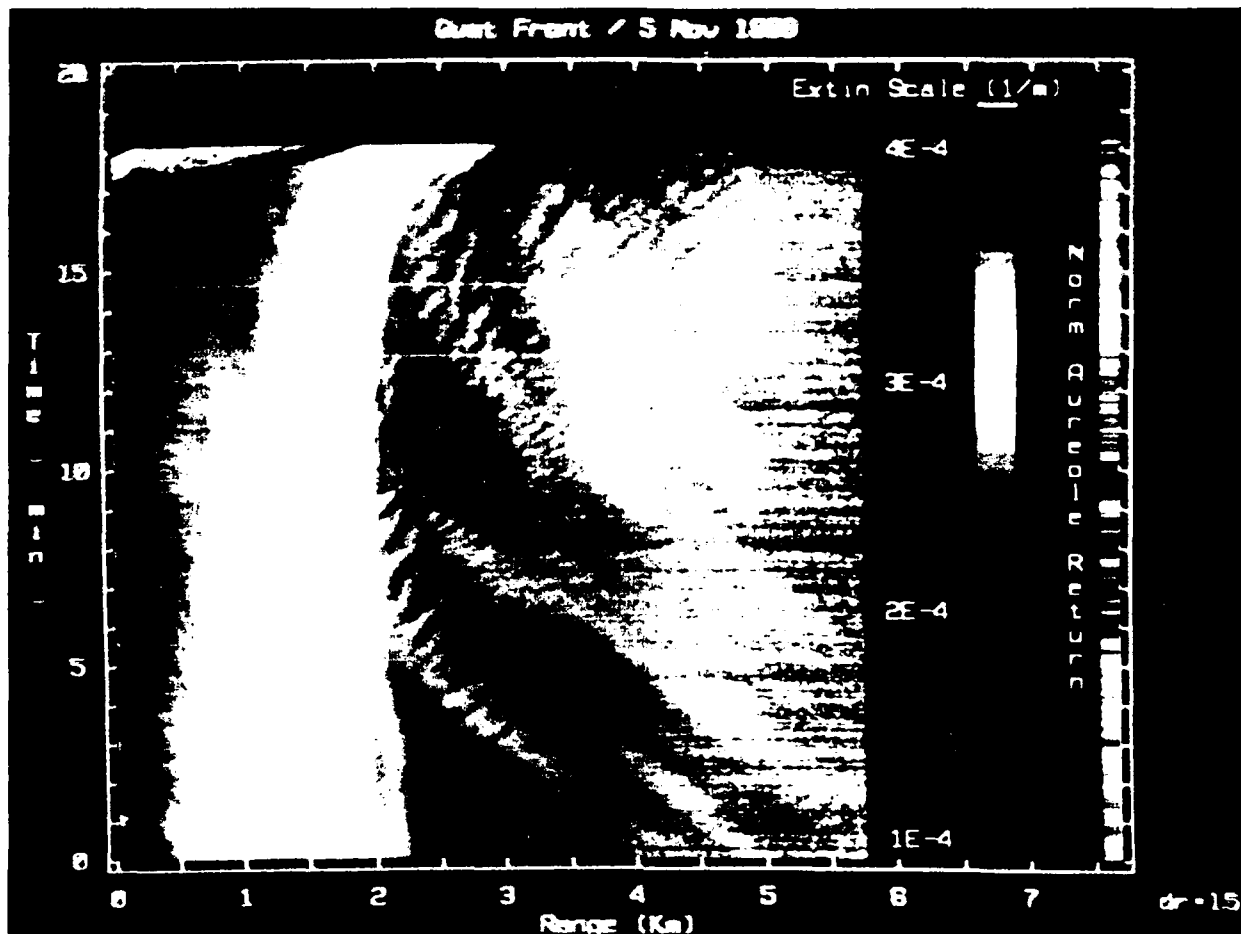


Figure 9. The lidar returns as a function of range and time is shown in false color. Zero range is at the lidar location and 5 km is in the middle of the Chesapeake Bay. Each false color represents a narrow range of extinction values. The blue and white shades are clear and hazy conditions respectively. The data was taken prior the passage of thunderstorm while the wind gusted to about 15 m/s and was directed along the lidar beam from the near lidar range to far range. The white band near the shore appears to be a large eddy caused by the bay shore cliff. The narrow bands beyond 2 km trace small scale eddies. Just before the end of the data session, the gust front proceeding the thunderstorm can be seen by the blue-white interface that moves from the near range out to far range. The red regions in the first few kilometers at the end of data is return from rain.